Theoretical and numerical Green's function field solution in a plane multilayered medium

F. R. DiNapoli and R. L. Deavenport

New London Laboratory, Naval Underwater System Center, New London, Connecticut 06320
(Received 2 October 1978; accepted for publication 4 October 1979)

An explicit general form is derived for the depth-dependent Green's function occurring in the integral solution to the Helmholtz wave equation for range-independent layered media. This representation permits arbitrary location of the source and receiver. In addition, a technique, the Fast Field Program (FFP), for the evaluation of the integral solution is delineated. Examples of the use of both the formulation and the FFP to the problem of modeling underwater acoustic propagation loss versus range, where the source/receiver are in air/water, in water/bottom, and in a cross-layer surface duct, are discussed.

PACS numbers: 43.30.Bp, 03.40.Kf, 43.20.Bi

INTRODUCTION

Wave motion in a plane stratified medium has been studied in many diverse fields. The techniques developed in one field, however, are often applicable to others. This is not surprising, since the waves (whether they are electomagnetic, acoustic, seismic, etc). have common mathematical denominators. Phenomena associated with wave propagation in a medium with nonuniform characteristic properties are of particular interest. Although they are, in general, a function of all spatial coordinates and time, the case of arbitrary variation in only one spatial direction is a sufficiently accurate assumption for many applications.

It is easy to express the formal solution for the field produced by a point monochromatic source imbedded in such a medium as a Fourier–Bessel transform[1] or, equivalently, a Green's function convolution.[2] However, the explicit general form for the kernel, which results when the index of refraction is a piecewise continuous function and, in addition, the source and field point depths are arbitrary, has not appeared in the literature to our knowledge. Previous treatments have considered either a specific variation in the index of refraction or have used source and field points that were within the same layer. Wait,[3] for example, uses the Fourier–Bessel method to generalize the Sommerfield problem to the case of m-homogeneous layers. Harkrider[4] and Kutschale[5] have also given integral solutions for this case. Felsen and Marcuvitz,[2] Wait,[3] and Brekhovskikh[6] give excellent accounts of the electromagnetic field within general stratified media, but their explicit results hold only when the source and field points are within the same layer.

The formal Green's function integral to the reduced wave equation in cylindrical coordinates is given in Sec. I for the case of piecewise layered media, and arbitrary source and receiver depths. The stated formalism pertains to the acoustic case but can be used to describe other types of wave propagation when the change in variables describes the characteristic properties of the medium. The integrand is defined as a product of a range, r-dependent Bessel function, and a depth, z-dependent Green's function. The derivation of the former is straightforward, since the index of refraction is independent of range. The result for the depth-dependent Green's function is complicated due to the piecewise nature assumed for the index of refraction.

Eigenfunction expansion solutions to this integral have been formulated.[1-6] Kutschale[5] gives a complete wave solution in terms of normal modes and branch line integrals for homogeneous layers, and Stickler[7] provides the complete solution when the square of the index of refraction in each layer is a linear function of depth. There are times, however, when it is computationally easier to deal directly with the integral solution, especially as new numerical integration techniques become available. Solutions of this nature require the explicit formulation provided in Sec. I. One such method is the Fast Field Program (FFP) conceived by Marsh[8] in 1967 and extended by DiNapoli,[9] which has proved useful in applications to underwater acoustic propagation. This technique is briefly summarized and used in conjunction with the results of Sec. I to evaluate several examples.

In Sec. II, the depth-dependent Green's function solution is derived when the index of refraction is a piecewise continuous function of z. The Green's function is constructed from fundamental solutions of the classical Sturm–Liouville differential equation with discontinuous coefficients by use of the matrizant (propagator) method.

I. FORMAL SOLUTION

A given stratified medium is approximated by $N-1$ inhomogeneous layers sandwiched between two homogeneous half-spaces as shown in Fig. 1. A point source of angular frequency ω [time factor of $\exp(-i\omega t)$ has been suppressed] is located at $(0, z_s)$ in the LSth layer, where $0 \leq LS \leq N$. The field point is located at (r, z) in the LRth layer, where $0 \leq LR \leq N$. It is assumed that $z \geq z_s$. When $z \leq z_s$, reciprocity is used.

The Helmholtz reduced wave equation for a point source located at $\bar{r}_s$ in an inhomogeneous medium is given by

$$\nabla^2 G + k_{\text{eff}}^2(z)\hat{G} = -i\omega\rho^{1/2}(z_s)S_\omega\delta(\bar{r}-\bar{r}_s). \quad (1)$$

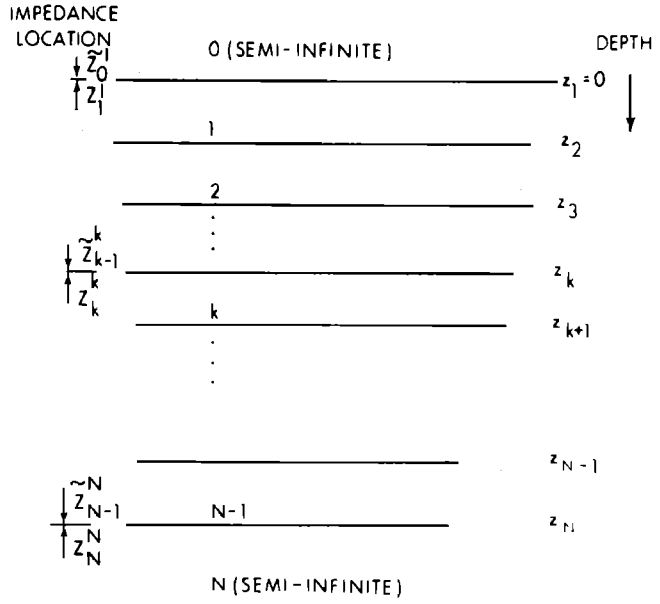

FIG. 1. Environmental description of stratified media.

The effective wavenumber $k_{eff}(z)$ is defined in terms of the usual wavenumber $k(z)[=\omega/\text{sound speed variation } c(z)]$ according to

$$k_{eff}^2(z)=k^2(z)-[\rho(z)]^{1/2}\frac{d^2}{dz^2}\left(\frac{1}{[\rho(z)]^{1/2}}\right), \tag{2}$$

where, for acoustics, $\rho(z)$ is the density. In electromagnetics, $\rho(z)$ may be either the dielectric parameter $\epsilon(z)$ or the permeability $\mu(z)$; in seismology, $\rho(z)$ is the Lamé parameter $\mu^{-1}(z)$, for SH propagation.

By the simple transformation $\Phi=\sqrt{\rho}\,\hat{G}$, Eq. (1) may be rewritten as

$$\nabla^2\Phi+k^2(z)\Phi-\nabla\rho\cdot\nabla\Phi/\rho=-i\omega\rho(z_s)S_\omega\delta(\bar{r}-\bar{r}_s), \tag{3}$$

where Φ represents the pressure at some point r due to the point source, and S_ω is the source strength defined by Morse and Ingard.[10] If cylindrical coordinates (r,θ,z) are assumed with azimuthal symmetry, the following equation is obtained:

$$\frac{1}{r}\frac{\partial}{\partial r}\left(r\frac{\partial\Phi}{\partial r}\right)+\rho(z)\frac{\partial}{\partial z}\left(\frac{1}{\rho(z)}\frac{\partial\Phi}{\partial z}\right)+k^2(z)\Phi$$
$$=\frac{-i\omega\rho(z_s)}{2\pi r}S_\omega\delta(r)\delta(z-z_s). \tag{4}$$

The vertical depth coordinate z varies from $-\infty\le z\le+\infty$ and the range coordinate r varies from $0<r<\infty$. The boundary conditions imposed on Eq. (4) are that Φ must satisfy radiation conditions for

$$r\to\infty \text{ and } z\to\pm\infty, \tag{5a}$$

$$i\omega\rho\Phi\left(\frac{\partial\Phi}{\partial z}\right)^{-1} \text{ and } \Phi \tag{5b}$$

must be continuous across all interfaces which are assumed to be parallel in the r direction. Equation (4) can be separated as

$$\left[\frac{d}{dr}\left(r\frac{d}{dr}\right)+\xi^2 r\right]G_r(r,\xi)=\frac{-\delta(r)S_\omega}{2\pi}, \tag{6}$$

$$\left[\rho(z)\frac{d}{dz}\left(\frac{1}{\rho(z)}\frac{d}{dz}\right)+k^2(z)-\xi^2\right]G(z,z_s;\xi)$$
$$=-i\omega\rho(z_s)\delta(z-z_s), \tag{7}$$

where ξ^2 is the separation constant. $G_r(r,\xi)$ is given by $iS_\omega/4$ times the Hankel function $H_0^{(1)}(\xi r)$, and $G(z,z_s;\xi)$ represents the depth-dependent Green's function.

The integral solution to the above boundary value problem can be given by the Fourier–Bessel transform,

$$\Phi(r,z,z_s)=\frac{S_\omega}{2\pi}\int_0^\infty G(z,z_s;\xi)J_0(\xi r)\xi\,d\xi, \tag{8}$$

first used by Sommerfeld[11] and Lamb[12] or by Green's function convolution,

$$\Phi(r,z,z_s)=\frac{S_\omega}{4\pi}\int_{\infty e^{+i\pi}}^{\infty} G(z,z_s;\xi)H_0^{(1)}(\xi r)\xi\,d\xi, \tag{9}$$

first described by Titchmarsh.[13]

Equations (8) and (9) represent the formal solution to our problem. Either representation can be used, since they may be transformed into one another.

There are many ways by which Eqs. (8) and (9) can be integrated. We will discuss only three. The first and most popular is the so-called residue method. In this method, Cauchy's residue theorem is used to evaluate the basic integral. The poles are given by the zeros of the Wronskian of the independent solutions used to construct $G(z,z_s;\xi)$. By using the residue theorem, the basic integral can be written as a summation over the residue contributions minus line integrals around any branch points. The residue contriubtions yield the eigenfunction expansion usually referred to as normal modes. This method has been very valuable in many wave propagation problems; for example, Lamb[12] and Sommerfeld[11] used it in their pioneering works, and additional insight has been provided by Brekhovskikh,[6] Tolstoy,[14] Wait,[3] and Felsen and Marcuvitz[2] in their books.

The multipath expansion technique is another method used to evaluate the basic integral solution. Van der Pol and Bremmer[15] seem to have been the first to study the expansion in detail, although Debye[16] had used it earlier. Wait[17] extended the method to allow for caustic regions and more recently further extensions to the basic work of Van der Pol and Bremmer have been made by Batorsky and Felsen,[18] Leibiger,[19] and Weinberg.[20] The latter workers have also developed computer programs utilizing the multipath expansion.

In the multipath expansion method, the denominator of $G(z,z_s;\xi)$ is expanded in a Taylor series which allows for the basic integral to be broken up into a series of simpler integrals which sometimes can be identified with certain ray paths. These ray path integrals are then generally evaluated by using stationary phase techniques or numerical schemes. The multipath method represents an approximate method when the series is truncated, and the effect of layering is only partially allowed for in the integration.

The last method for evaluating the basic integral will

be the Fast Field Program (FFP). The FFP was developed by Marsh and DiNapoli[8,9] and makes use of the Fast Fourier Transform (FFT) to directly integrate Eq. (8). The first step in this method consists of replacing the Bessel function in the integral solution of Eq. (8) with the Hankel function associated with outward propagation. [The integral involving $H_0^{(2)}(\xi r)$ does not contribute significantly and is neglected. An example comparing the results from Eq. (8) with those obtained from using only $H_0^{(1)}$ is provided in Appendix B, Example B2.] If the first term in its asymptotic expansion,

$$H_0^{(1)}(\xi r) \simeq \left(\frac{2}{\pi i}\right)^{1/2} \frac{e^{i\xi r}}{(\xi r)^{1/2}} , \tag{10}$$

is then substituted, Eq. (8) may be written as

$$\mathcal{P}(r,z,z_s) \simeq \left(\frac{2}{\pi i}\right)^{1/2} \frac{S_\omega}{4\pi} \int_0^\infty \left(\frac{\xi}{r}\right)^{1/2} G(z,z_s;\xi) e^{i\xi r} d\xi . \tag{11}$$

Next, let the horizontal wavenumber ξ and the horizontal range r be evaluated at the discrete values.

$$\xi_m = \xi_0 + m\Delta\xi, \quad r_n = r_0 + n\Delta r ,$$
$$(m,n) = 0,1,2,\ldots,L-1 , \tag{12}$$

with the added restriction that

$$\Delta r \Delta\xi = 2\pi/L , \tag{13}$$

where L is equal to 2 raised to some integer power. Equation (11) is then given by

$$\mathcal{P}(r_n,z,z_s) \simeq \Delta\xi \left(\frac{2}{\pi i}\right)^{1/2} \frac{S_\omega}{4\pi} \frac{e^{i\xi_0 r_n}}{r_n^{1/2}} \sum_{m=0}^{L-1} E_m e^{i2\pi mn/L} , \tag{14}$$

where the input to the FFT is

$$E_m = G(z,z_s;\xi_m)\xi_m^{1/2} e^{im r_0 \Delta\xi} . \tag{15}$$

Equation (14) is now in a form that is directly amenable to the FFT. The result of the application of the FFT is the value of the field at each of the n discrete ranges which are obtained essentially simultaneously. This format is thus ideally suited for the rapid calculation of the field as a function of range, and proceeds very rapidly once the input [Eq. (15)] is obtained.

II. DEPTH-DEPENDENT GREEN'S FUNCTION

From Eq. (7), the depth-dependent Green's function $G(z,z_s)$ must satisfy

$$\mathcal{L}(G) = \frac{d}{dz}\left(\frac{1}{i\omega\rho(z)} \frac{dG}{dz}\right) + q(z)G = -\delta(z-z_s) , \tag{16}$$

where $q(z) = [k^2(z) - \xi^2]/[i\omega\rho(z)]$. The differential operator $\mathcal{L}$ is defined as

$$\mathcal{L} = \frac{d}{dz}\left(\frac{1}{i\omega\rho(z)} \frac{d}{dz}\right) + q(z) .$$

The solution of Eq. (16) is found by using the matrizant method of Refs. 21–24 to obtain two linearly independent functions, $\tilde{F}$ and F, which satisfy Eq. (16) for $z < z_s$ and $z > z_s$ and the respective continuity conditions of Eq. (5b) on G and $(dG/dz)/i\omega\rho(z)$, $\{= G'(z)/[i\omega\rho(z)]\}$ in those regions. These functions represent the depth-dependent pressure and are unique, up to an arbitrary constant, which may be chosen such that Eq. (16) is also satisfied at the source depth z_s.

The notation used in this article was instituted to conserve space. Although compact, it is unorthodox, and will be explained whenever it is felt that confusion might arise. The symbol U without a subscript or superscript is an abbreviation for the depth-dependent particle velocity $U = (dF/dz)/[i\omega\rho(z)]$, for $z > z_s$. When it appears with a subscript and superscript, e.g., U_k^{k+1}, the subscript (k) refers to the layer in which F is defined. The superscript $(k+1)$ refers to the depth (z_{k+1}, see Fig. 1) at which the operation is evaluated. Thus

$$U_k^{k+1} = \frac{1}{i\omega\rho_k(z)} \frac{dF_k}{dz}\bigg|_{z=z_{k+1}}$$

and as such U_k^{k+1} is the depth-dependent particle velocity in the kth layer evaluated at the depth z_{k+1}. If the subscript is absent and the superscript is z, then U^z is the depth-dependent particle velocity in any layer ($LS \leq k \leq N-1$) evaluated at any depth ($z_s < z \leq z_N$). The depth-dependent particle velocity $\tilde{U} = (d\tilde{F}/dz)/[i\omega\rho(z)]$ for $z < z_s$ is abbreviated similarly. Functions other than the depth-dependent particle velocity will appear with a subscript and superscript (e.g., γ_k^{k+1}). The meaning of the subscript and superscript when it occurs with these functions will be exactly the same as that explained above for U, unless otherwise stated.

Terms of the form $(df/dz)/[i\omega\rho(z)]$ and $(dg/dz/[i\omega\rho(z)]$ appeared frequently throughout the analysis and have been abbreviated as (Df) and (Dg), respectively. Thus

$$(Df)_k^{k+1} = \frac{1}{i\omega\rho_k(z)} \frac{df_k}{dz}\bigg|_{z=z_{k+1}} .$$

Although closely related to the depth-dependent particle velocity U_k^{k+1}, they differ from it because the function being operated on is not the total depth-dependent pressure, but one of the linearly independent (fundamental) solutions used to form F.

The equation for the depth-dependent pressure F, $z > z_s$, may be written as

$$\mathcal{L}(F) = \frac{d}{dz}\left(\frac{1}{i\omega\rho(z)} \frac{dF}{dz}\right) + q(z)F = 0 , \tag{17}$$

where F is subject to the continuity conditions of Eq. (5b) for $z > z_s$. In the matrizant method, Eq. (17) is written as the two equations

$$U(z) = \frac{1}{i\omega\rho(z)} \frac{dF}{dz} ; \quad \frac{dU}{dz} + q(z)F = 0 , \tag{18}$$

or equivalently as the matrix equation

$$\frac{d\psi(z)}{dz} = A(z)\psi(z) , \tag{19}$$

where

$$\psi(z) = \begin{bmatrix} F(z) \\ U(z) \end{bmatrix}; \quad A(z) = \begin{bmatrix} 0 & i\omega\rho(z) \\ -q(z) & 0 \end{bmatrix} .$$

The solution of Eq. (19) satisfying initial conditions at z_i is given by

$$\psi(z) = \tilde{M}(z,z_i)\psi(z_i) , \tag{20}$$

where $\bar{M}(z,z_i)$ is the fundamental matrix (matrizant, propagator, state transition matrix, etc.) which satisfies the matrix equation.

$$\frac{d\bar{M}(z,z_i)}{dz}=A(z)\bar{M}(z,z_i)\,, \tag{21}$$

such that $\bar{M}(z_i,z_i)=I$, where I is the identity matrix.

When the entire interval $[z_1,z_N]$ is considered as a single layer the matrizant can be calculated by various techniques, such as Volterra's product integral,[23,24] or the Peano–Baker expansion.[21,25] An alternate method for evaluating $\bar{M}$ is to subdivide the total interval $[z_1,z_N]$ into $N-1$ subintervals, $(z_1<z_2<\ldots<z_i<z_{i+1}<\ldots<z_N)$ as in Fig. 1. Within each subinterval $k(z)$ is replaced by a continuous function $k_i(z)$ which is a good approximation to $k(z)$ over $[z_i,z_{i+1}]$. The function $k_i(z)$ is chosen such that fundamental solutions $f(\gamma^z)$ and $g(\gamma^z)$ of $\mathcal{L}(\cdot)=0$ over $[z_i,z_{i+1}]$ can be expressed in terms of known solutions. The known solutions satisfy a linear second-order differential equation whose independent variable $\gamma^z[=\gamma(z)]$ is a function of z. The matrizant

$$\bar{M}(z,z_i)=M(\gamma^z,\gamma^{z_i})=\begin{bmatrix}Q(\gamma^z,\gamma^{z_i}) & P(\gamma^z,\gamma^{z_i})\\ S(\gamma^z,\gamma^{z_i}) & R(\gamma^z,\gamma^{z_i})\end{bmatrix} \tag{22}$$

over some arbitrary subinterval $[z,z_i]$ may then be expressed as

$$M(\gamma^z,\gamma^{z_i})=\begin{bmatrix}f(\gamma^z) & g(\gamma^z)\\ (Df)^z & (Dg)^z\end{bmatrix}\begin{bmatrix}f(\gamma^{z_i}) & g(\gamma^{z_i})\\ (Df)^{z_i} & (Dg)^{z_i}\end{bmatrix}^{-1}. \tag{23}$$

The use of the argument γ^z is intended as a visual reminder that f and g are to be expressed in terms of known solutions. The matrizant for the entire interval can then be obtained by making use of its group property

$$M(\gamma^z,\gamma^{z_i})=M(\gamma^z,\gamma^{z_k})M(\gamma^{z_k},\gamma^{z_i})\,,\quad z,z_i,z_k\in[z_1,z_N]\,, \tag{24}$$

and $M^{-1}(\gamma^z,\gamma^{z_i})=M(\gamma^{z_i},\gamma^z)$. From Eq. (23), the elements of Eq. (22) are

$$\begin{aligned}
&Q(\gamma^z,\gamma^{z_i})=\frac{[f(\gamma^z)(Dg)^{z_i}-(Df)^{z_i}g(\gamma^z)]}{[f(\gamma^{z_i})(Dg)^{z_i}-(Df)^{z_i}g(\gamma^{z_i})]}\,,\\
&Q(\gamma^{z_i},\gamma^{z_i})=1\,,\\
&R(\gamma^z,\gamma^{z_i})=\frac{[-(Df)^zg(\gamma^{z_i})+(Dg)^zf(\gamma^{z_i})]}{[f(\gamma^{z_i})(Dg)^{z_i}-(Df)^{z_i}g(\gamma^{z_i})]}\,,\\
&R(\gamma^{z_i},\gamma^{z_i})=1\,,\\
&S(\gamma^z,\gamma^{z_i})=\frac{[(Df)^z(Dg)^{z_i}-(Df)^{z_i}(Dg)^z]}{[f(\gamma^{z_i})(Dg)^{z_i}-(Df)^{z_i}g(\gamma^{z_i})]}\,,\\
&S(\gamma^{z_i},\gamma^{z_i})=0\,,\\
&P(\gamma^z,\gamma^{z_i})=\frac{[-f(\gamma^z)g(\gamma^{z_i})+g(\gamma^z)f(\gamma^{z_i})]}{[f(\gamma^{z_i})(Dg)^{z_i}-(Df)^{z_i}g(\gamma^{z_i})]}\,,\\
&P(\gamma^{z_i},\gamma^{z_i})=0\,.
\end{aligned} \tag{25}$$

The Green's function solution to Eq. (16) can now be constructed from the following two matrizant equations:

$$\begin{aligned}
\begin{bmatrix}G(z)\\ \dot{G}(z)/[i\omega\rho(z)]\end{bmatrix}&=\tilde{\psi}(z)=\begin{bmatrix}\tilde{F}(z)\\ \tilde{U}(z)\end{bmatrix}\\
&=M(\gamma^z,\gamma^{z_1})\tilde{\psi}(z_1)\,,\quad(z_1\le z<z_s)\,,\\
\begin{bmatrix}G(z)\\ \dot{G}(z)/[i\omega\rho(z)]\end{bmatrix}&=\psi(z)=\begin{bmatrix}F(z)\\ U(z)\end{bmatrix}\\
&=M(\gamma^z,\gamma^{z_N})\psi(z_N)\,,\quad(z_s<z\le z_N)\,,
\end{aligned} \tag{26}$$

where z_1 and z_N represent the lower and upper boundaries (see Fig. 1), respectively, of two homogeneous half-spaces between which the index of refraction is allowed be a piecewise continuous function of z. The initial values are thus known up to some multiplicative constants, a_0 and a_N, respectively, since

$$\begin{aligned}
&\tilde{F}(z)=a_0e^{-i\beta_0(z-z_1)}\,,\quad \tilde{U}(z)=\frac{-\beta_0}{\omega\rho_0(z)}\tilde{F}(z)\,,\quad z<z_1\,,\\
&F(z)=a_Ne^{i\beta_N(z-z_N)}\,,\quad U(z)=\frac{\beta_N}{\omega\rho_N(z)}F(z)\,,\ z>z_N\,,
\end{aligned} \tag{27}$$

where β_0 and β_N are the z components of the wavenumbers k_0 and k_N, respectively, and $\mathrm{Im}\{\beta_0\}$ and $\mathrm{Im}\{\beta_N\}>0$ are required to satisfy the radiation conditions of Eq. (5a).

In what follows it is useful to rewrite $\tilde{\psi}(z)$ and $\psi(z)$ in terms of the impedance $\tilde{Z}$ above the source and Z below the source defined as

$$\tilde{Z}(z)=\frac{\tilde{F}(z)}{\tilde{U}(z)}\ \text{and}\ Z(z)=\frac{F(z)}{U(z)}\,, \tag{28}$$

since the terminal impedances

$$Z_N^N=\frac{\omega\rho_N}{\beta_N}\ \text{and}\ \tilde{Z}_0^1=\frac{-\omega\rho_0}{\beta_0} \tag{29}$$

are known uniquely. The convention adopted is that the superscript always refers to the depth at which Z is evaluated and the subscript to the layer where the evaluation takes place. Then the impedance anywhere above the source can be written uniquely in terms of its terminal impedance $\tilde{Z}_0^1$ by using the group property of Eq. (24) to obtain

$$\begin{bmatrix}\tilde{Z}_k^z\\ \cdot\\ 1\end{bmatrix}=\frac{M_k(\gamma_k^z,\gamma_k^k)\left[\prod_{\rho=k-1}^{1}M_\rho(b,a)\right]\begin{bmatrix}\tilde{Z}_0^1\\ 1\end{bmatrix}}{[\tilde{Z}_{k-1}^kS_k(\gamma_k^z,\gamma_k^k)+R_k(\gamma_k^z,\gamma_k^k)]\prod_{\rho=k-1}^{1}[\tilde{Z}_{\rho-1}^\rho S_\rho(b,a)+R_\rho(b,a)]} \tag{30}$$

and similarly below the source

$$\begin{bmatrix}Z_k^z\\ 1\end{bmatrix}=\frac{M_k(\gamma_k^z,\gamma_k^{k+1})\left[\prod_{\rho=k+1}^{N-1}M_\rho(a,b)\right]\begin{bmatrix}Z_N^N\\ 1\end{bmatrix}}{[Z_{k+1}^{k+1}S_k(\gamma_k^z,\gamma_k^{k+1})+R_k(\gamma_k^z,\gamma_k^{k+1})]\prod_{\rho=k+1}^{N-1}[Z_{\rho+1}^{\rho+1}S_\rho(a,b)+R_\rho(a,b)]}\,, \tag{31}$$

where $a=\gamma_p^p$, $b=\gamma_p^{p+1}$ are evaluated at the upper and lower boundaries of the pth layer, respectively. The symbols a, b will be used as abbreviations for the arguments throughout, except where explicitly noted to the contrary. The continuity of impedance at the boundaries between z_1 and z_N is automatically satisfied from the imposed condition that $\bar{M}(z_i, z_i)$ be the identity matrix.

The matrix $\bar{\psi}_k(z)$ in the kth layer above the source may now be expressed as

$$\bar{\psi}_k(z)=M_k(\gamma_k^z,\gamma_k^{k+1})\begin{bmatrix}\tilde{Z}_k^{k+1}\\1\end{bmatrix}\tilde{U}_k^{k+1}, \tag{32}$$

where $z_k \le z \le z_{k+1}$ for $1 \le k \le LS-1$, and $z_{LS} \le z < z_s$ for $k=LS$, the source layer. Applying Eq. (24) over $[z_{k-1}, z_{k+1}]$ yields

$$\tilde{U}_k^{k+1}=\tilde{U}_{k-1}^k[\tilde{Z}_{k-1}^k S_k(b,a)+R_k(b,a)], \quad a=\gamma_k^k \text{ and } b=\gamma_k^{k+1}. \tag{33}$$

Thus Eq. (32) may be written as

$$\bar{\psi}_k(z)=M_k(\gamma_k^z,\gamma_k^{k+1})\begin{bmatrix}\tilde{Z}_k^{k+1}\\1\end{bmatrix}[\tilde{U}_{k-1}^k(\tilde{Z}_{k-1}^k S_k(b,a)+R_k(b,a)]. \tag{34}$$

Likewise the matrix $\psi_k(z)$ below the source may be expressed as

$$\psi_k(z)=M_k(\gamma_k^z,\gamma_k^{k+1})\begin{bmatrix}Z_{k+1}^{k+1}\\1\end{bmatrix}U_{k+1}^{k+1}, \tag{35}$$

where $z_k \le z \le z_{k+1}$ for $LS+1 \le k \le N-1$ and $z_{LS+1} \ge z > z_s$ for $k=LS$. The impedances $\tilde{Z}_k^{k+1}$ and Z_{k+1}^{k+1} are the terminal impedances $\tilde{Z}_0$ and Z_N^N referenced to the bottom of the kth layer and may be easily found from Eqs. (30) and (31). The Green's function in the kth layer for $z < z_s$ may now be written as

$$G_k(z)=[\tilde{Z}_k^{k+1}Q_k(\gamma_k^z,\gamma_k^{k+1})+P_k(\gamma_k^z,\gamma_k^{k+1})] \times\{\tilde{U}_{k-1}^k[\tilde{Z}_{k-1}^k S_k(b,a)+R_k(b,a)]\}. \tag{36}$$

Similarly, the Green's function in the kth layer for $z > z_s$ is

$$G_k(z)=[Z_{k+1}^{k+1}Q_k(\gamma_k^z,\gamma_k^{k+1})+P_k(\gamma_k^z,\gamma_k^{k+1})]U_{k+1}^{k+1}. \tag{37}$$

The subscript on $G_k(z)$ will generally be omitted since the receiver is always located at (r,z) in the LRth layer.

Thus the Green's function $G(z), z<z_s$, may be written in terms of $\tilde{Z}_k^{k+1}$, and the multiplicative constant $\tilde{U}_{k-1}^k[\tilde{Z}_{k-1}^k S_k(b,a)+R_k(b,a)]$. Similarly $G(z), z>z_s$ is given in terms of Z_{k+1}^{k+1} and the constant U_{k+1}^{k+1}. Since the local terminal impedances Z_k^{k+1} and Z_{k+1}^{k+1} are uniquely determined from Eqs. (30) and (31) in terms of the known half-space impedances $\tilde{Z}_0^1$ and Z_N^N, respectively, the Green's function $G(z)$ is completely specified upon determination of the multiplicative constants.

If continuity of $\tilde{F}_k$ and $\tilde{U}_k$ is to hold everywhere above the source, then $\bar{\psi}_k(z_k)=\bar{\psi}_{k-1}(z_k)$ or, equivalently, $\tilde{U}_{k-1}^k[\tilde{Z}_{k-1}^k S_k(b,a)+R_k(b,a)]=\tilde{U}_k^{k+1}$. The relation to the constant in the source layer is for $1 \le k \le LS-1$.

$$U_{k-1}^k[\tilde{Z}_{k-1}^k S_k(b,a)+R_k(b,a)] = \frac{\tilde{U}_{LS-1}^{LS}[\tilde{Z}_{LS-1}^{LS}S_{LS}(\gamma_{LS}^{LS+1},\gamma_{LS}^{LS})+R_{LS}(\gamma_{LS}^{LS+1},\gamma_{LS}^{LS})]}{\prod_{p=k+1}^{LS}[\tilde{Z}_{p-1}^p S_p(b,a)+R_p(b,a)]}. \tag{38}$$

Similarly, if continuity of F_k and U_k is to hold everywhere below the source,

$$\psi_k(z_{k+1})=\psi_{k+1}(z_{k+1})$$

or

$$U_{k+1}^{k+1}=U_k^k/[Z_{k+1}^{k+1}S_k(a,b)+R_k(a,b)].$$

This may be written in terms of the source constant as

$$U_{k+1}^{k+1}=\frac{U_{LS+1}^{LS+1}}{\prod_{p=LS+1}^{k}[Z_{p+1}^{p+1}S_p(a,b)+R_p(a,b)]}, \quad LS+1 \le k \le N-1. \tag{39}$$

The two constants $\tilde{U}_{LS}^{LS-1}$ and U_{LS+1}^{LS+1} are determined by integrating Eq. (16) between the limits $z_s-\epsilon$ and $z_s+\epsilon$, and taking the limit as ϵ goes to zero. This is equivalent to satisfying the source conditions,

$$F_{LS}^S-F_{LS}^S=0, \quad U_{LS}^S-\tilde{U}_{LS}^S=-1.$$

The superscript S denotes that the evaluation occurs at the source depth z_s. One finds that the above conditions will be satisfied if the constants are defined according to

$$U_{LS+1}^{LS+1}=a_{12}/W,$$
$$\tilde{U}_{LS-1}^{LS}[\tilde{Z}_{LS-1}^{LS}S_{LS}(b,a)+R_{LS}(b,a)]=a_{11}/W, \tag{40}$$

where with $e=\gamma_{LS}^S$, $a=\gamma_{LS}^{LS}$, and $b=\gamma_{LS}^{LS+1}$,

$$a_{11}=(Z_{LS+1}^{LS+1}\,1)\begin{bmatrix}Q_{LS}(e,b)\\P_{LS}(e,b)\end{bmatrix},$$
$$a_{12}=[Q_{LS}(e,b)\,P_{LS}(e,b)]\begin{bmatrix}\tilde{Z}_{LS}^{LS+1}\\1\end{bmatrix}, \tag{41}$$

and the Wronskian is found to be given by

$$W=Z_{LS+1}^{LS+1}-\tilde{Z}_{LS}^{LS+1}, \tag{42}$$

the difference between the terminal impedance Z_N^N referenced up to the level $z=z_{LS+1}$ and the terminal impedance $\tilde{Z}_0^1$ referenced down to that same level. The constants in each layer are then

$$[\tilde{Z}_{k-1}^k S_k(b,a)+R_k(b,a)]\tilde{U}_k^{k-1} = \left[\frac{a_{11}}{W}\right]\left[\prod_{p=k+1}^{LS}[\tilde{Z}_{p-1}^p S_p(b,a)+R_p(b,a)]\right]^{-1}, \quad 1 \le k \le LS-1, \tag{43}$$

and

$$U_{k+1}^{k+1}=\left[\frac{a_{12}}{W}\right] \Big/ \prod_{p=LS+1}^{k}[Z_{p+1}^{p+1}S_p(a,b)+R_p(a,b)], \quad LS+1 \le k \le N-1. \tag{44}$$

Thus $G(z,z_s)$ in any layer can be found by using these constants in Eqs. (36) and (37). If both the source and receiver are in the same layer (i.e., $LS=LR$), the Green's function for $z_{LS} \le z \le z_s$ and $1 \le LS \le N-1$ is

$$G(z,z_s)=\frac{[\tilde{Z}_{LR}^{LR+1}Q_{LR}(\gamma_{LR}^z,\gamma_{LR}^{LR+1})+P_{LR}(\gamma_{LR}^z,\gamma_{LR}^{LR+1})][Z_{LS+1}^{LS+1}Q_{LS}(\gamma_{LS}^S,\gamma_{LS}^{LS+1})+P_{LS}(\gamma_{LS}^S,\gamma_{LS}^{LS+1})]}{Z_{LS+1}^{LS+1}-\tilde{Z}_{LS}^{LS+1}}. \tag{45}$$

The solution valid for $z_s \leq z \leq z_{LS+1}$ is obtained by interchanging z and z_s in the above equation.

If the receiver is below the source and in a different layer (i.e., $LR > LS$), the Green's function for $z_{LR} \leq z \leq z_{LR+1}$, $LS+1 \leq LR \leq N-1$ is

$$G(z,z_s)=\frac{[Z_{LR+1}^{LR+1}Q_{LR}(\gamma_{LR}^{z},\gamma_{LR}^{LR+1})+P_{LR}(\gamma_{LR}^{z},\gamma_{LR}^{LR+1})][\tilde{Z}_{LS}^{LS+1}Q_{LS}(\gamma_{LS}^{S},\gamma_{LS}^{LS+1})+P_{LS}(\gamma_{LS}^{S},\gamma_{LS}^{LS+1})]\Delta_{LS+1}^{LR}}{Z_{LS+1}^{LS+1}-\tilde{Z}_{LS}^{LS+1}} \tag{46}$$

where

$$\Delta_{LS+1}^{LR}=\left(\prod_{k=LS+1}^{LR}[Z_{k+1}^{k+1}S_k(a,b)+R_k(a,b)]\right)^{-1}.$$

The form of the solution for G provided above is the familiar way of expressing the Green's function solution. Felsen and Marcuvitz[2] and also Coddington and Levinson[26] provide solutions which are identical in form to Eq. (46), except for the absence of the factor Δ_{LS+1}^{LR}. This factor is absent if both the source and receiver are in the same layer ($LS=LR$), as can be seen by examining Eq. (45). Thus the above result represents an extension of this earlier work in that the source and receiver may be in different layers in a piecewise layered media. The results for either LS or LR equal to zero or N are special cases from a notational standpoint only. The Green's function for these cases is provided in Appendix A.

The Green's function in the LRth layer may be expressed in various alternative forms, using the relations provided in this section. One such form which displays the dependence on the known terminal impedances Z_N^N and $\tilde{Z}_0^1$ explicitly is found to be

$$G(z,z_s)=\frac{(1-\tilde{Z}_0^1)K_1^{LS}\Phi_{LS}\Phi_{LR}K_{LR+1}^{N-1}\begin{bmatrix}Z_N^N\\1\end{bmatrix}}{(1-\tilde{Z}_0^1)K_1^{N-1}\begin{bmatrix}Z_N^N\\1\end{bmatrix}}, \tag{47}$$

where $z_{LR} \leq z \leq z_{LR+1}$ for $LS+1 \leq LR \leq N-1$ and $z_s \leq z \leq z_{LS+1}$. All the terms in the above expression are matrices. In particular,

$$\Phi_{LS}=\begin{bmatrix}P_{LS}(\gamma_{LS}^{S},\gamma_{LS}^{LS+1})\\-Q_{LS}(\gamma_{LS}^{S},\gamma_{LS}^{LS+1})\end{bmatrix},$$

$$\Phi_{LR}=[(Q_{LR}(\gamma_{LR}^{z},\gamma_{LR}^{LR+1})\,P_{LR}(\gamma_{LR}^{z},\gamma_{LR}^{LR+1})],$$

$$K_1^p=\prod_{k=1}^{p}M_k(\gamma_k^k,\gamma_k^{k+1}). \tag{48}$$

The expression for $G(z,z_s)$ valid above the source is obtained from Eq. (47) by interchanging LS and LR, also z_s and z.

III. NUMERICAL CONSIDERATIONS

The only restriction imposed upon the matrizant of Sec. II was that the sound speed variation $C_k(z)$ associated with the known solutions be a good approximation to the given sound speed variation within the subinterval $z_k \leq z \leq z_{k+1}$. The solution for the pressure field by means of the FFT [Eq. (14)] necessitates the evaluation of the depth-dependent Green's function [Eq. (47)] for each of the L equispaced, discrete L values $\xi_m (m=0,1,2,\ldots,L-1)$ of the horizontal component of the wavenumber. This calculation represents the major portion of the required execution time. Thus the particular manner in which f_k, g_k depend upon ξ will have a strong bearing upon the ease with which G can be found as a function of ξ_m. Consideration of a few possible choices for the fundamental solutions will illustrate the point.

Trigonometric functions: $C_k(z)=a_k, z_k \leq z \leq z_{k+1}$

$$f_k(\gamma_k^{z},\xi_m)=\sin\gamma_k^{z},\quad g_k(\gamma_k^{z},\xi_m)=\cos\gamma_k^{z},$$

where

$$\gamma_k^{z}=(z_k-z)[(\omega/a_k)^2-\xi_m^2]^{1/2}.$$

The evaluation of a square root and a trigonometric function is required for each of the L values of ξ_m.

Airy function: $C_k^{-2}(z)=a_k+b_k(z_k-z), z_k \leq z \leq z_{k+1}$

$$f_k(\gamma_k^{z},\xi_m)=A_i(\gamma_k^{z}),\quad g_k(\gamma_k^{z},\xi_m)=B_i(\gamma_k^{z}),$$

where

$$\gamma_k^{z}=-L_k^2[\omega^2C_k^{-2}(z)-\xi_m^2],\quad L_k^2=\omega^{-4/3}b_k^{-2/3}.$$

The Airy functions must be recalculated L times.

In contrast to the above, allow the sound speed to vary exponentially within each layer according to

$$C_k(z)=a_ke^{(z-z_k)/H_k};\quad z_k \leq z \leq z_{k+1},\quad 1 \leq k \leq N-1,$$

where a_k is the sound speed at the top of the kth layer, which need not equal $C_{k-1}(z_k)$, and H_k is an arbitrary scale factor. The fundamental solutions are then found to be

$$f_k(\gamma_k^{z};\xi_m)=J_{(\nu_k)_m}(\gamma_k^{z}),\quad g_k(\gamma_k^{z};\xi_m)=\mathcal{V}_{(\nu_k)_m}(\gamma_k^{z}), \tag{49}$$

that is, cylindrical functions of complex order

$$(\nu_k)_m \simeq (\xi_mH_k-i\alpha H_k),$$

where α represents the value for attenuation in the medium and real argument

$$\gamma_k^{z}=\frac{\omega H_k}{C_k(z)};\quad \frac{d\gamma_k^{z}}{dz}=\frac{\gamma_k^{z}}{H_k}. \tag{50}$$

The dependence upon ξ_m can then be efficiently found by evaluating Eq. (49) once for a pair of starting values, say $(\nu_k)_0$, $(\nu_k)_1$, and utilizing the recurrence relations

$$Q_{\nu+1}=\left[\frac{b\rho_a}{a\rho_b}\right]R_\nu-\left[\frac{b}{a\rho_b}\right]\nu P_\nu+\left[\frac{b}{a\rho_b}\right](\nu+1)P_{\nu+1},$$

$$R_{\nu+1}=\left[\frac{a\rho_b}{b\rho_a}\right]Q_\nu+\left[\frac{a}{b\rho_a}\right]\nu P_\nu-\left[\frac{(\nu+1)}{\rho_a}\right]P_{\nu+1},$$

$$P_{\nu+2}=P_\nu+\frac{2(\nu+1)}{ab}\left[\rho_b Q_{\nu+1}-\rho_a R_{\nu+1}\right],$$

$$S_{\nu+1}=-\left[\frac{ab}{\rho_a\rho_b}\right]P_{\nu+2}+(\nu+1)\left[\frac{Q_{\nu+1}}{\rho_a}-\frac{R_{\nu+1}}{\rho_b}\right]+\left[\frac{(\nu+1)^2}{\rho_a\rho_b}\right]P_{\nu+1}, \tag{51}$$

where $\rho_a=i\omega H_k\rho_k(z_k)$, $\rho_b=i\omega H_k\rho_k(z_{k+1})$, and the arguments of the matrizant elements, which have been suppressed for notational convenience, are as in Sec. II,

$$a=\gamma_k^k,\quad b=\gamma_k^{k+1}.$$

The recurrence relations [Eq. (51)] are stable except when the $|\nu|$ falls between the arguments a,b. A discussion of their use in this situation is provided by DiNapoli and Powers.[27]

The wavenumber domain sampling distance $\Delta\xi$ is found to be

$$\Delta\xi=1/H_k, \tag{52}$$

upon noting that the recurrence relations require that the change in ν be unity. The fact that the FFT requires equispaced values of ξ_m is in conflict with Eq. (52), since H_k is different for each of the $(N-1)$ possible layers. Then let $\Delta\xi$ equal the reciprocal of the largest scale factor $H_{\max}$,

$$\Delta\xi=1/H_{\max}, \tag{53}$$

and restrict the remaining scale factors to some arbitrary integer multiple p_k of this value, i.e.,

$$H_{\max}/H_k=p_k,\quad k=1,2,\ldots,N-1. \tag{54}$$

This restriction limits the ability to approximate the given sound speed variation arbitrarily close but leaves enough flexibility to model most cases of interest in underwater acoustics. Then if the discrete values of ξ_m are given by

$$\xi_m=\xi_0+m\Delta\xi,\quad m=0,1,2,\ldots,L-1,$$

they yield the discrete values of the order of the cylindrical functions in each layer

$$(\nu_k)_m=(\xi_0H_k-i\alpha H_k)+m/p_k,\quad m=0,1,2,\ldots,L-1,\quad 1\leq k\leq N-1.$$

The condition that the change in ν_k be unity can be satisfied if p_k pairs of starting values are calculated and used in the recurrence relations.

The required computer memory for each layer with exponential sound speed is then $2p_k$ complex values of $P_{(\nu)_k}$ and p_k complex values for both $Q_{(\nu)_k}$ and $R_{(\nu)_k}$. [The values for $S_{(\nu)_k}$ can be obtained from Eq. (26).] For some m, the appropriate values of $P_{(\nu_k)_m}$, $Q_{(\nu_k)_m}$, and $R_{(\nu_k)_m}$ (where $1\leq k\leq N-1$) are selected and used to calculate Eq. (48). That result is stored in a complex array of size L and Eqs. (51) are used again for $m+1$.

Since the minimum value of ξ should be zero and we can show that $G(z,z_1;\xi)$ decays when $\xi>\omega/C_{\min}$, where $C_{\min}$ is the minimum sound speed within the region $z_1\leq z\leq z_N$, we find that the number of sample points L needed is approximately

$$L\sim(\omega/C_{\min})H_{\max}. \tag{55}$$

Typically $H_{\max}\sim10.^5$; hence not only does the number of calculations increase at high frequencies but also the available core storage may be exceeded. A technique has been implemented[28] for rigorously circumventing the core storage problem when it arises. Although the execution time and storage requirements increase with increasing frequency, the solution remains equally valid and accurate.

The only remaining point involves the accuracy of replacing the Hankel function $H_0^1(\xi r)$ with the first term in its asymptotic expansion, which was introduced without justification in the Introduction. A discussion of this approximation is provided in Appendix B.

IV. EXAMPLES

In this section, the results for the pressure field, plotted in terms of propagation loss versus range, are provided for three examples. The source and receiver locations have been purposely chosen at unusual depths in two of the examples to illustrate the generality of the formalism given in Sec. II. For the third example, the source is in a surface duct; the receiver is below the duct; and a relatively high frequency has been chosen to illustrate the general applicability of the FFP algorithm.

The same environmental description is used for all three examples. A plot of sound speed versus depth is provided in Fig. 2, with additional information given in

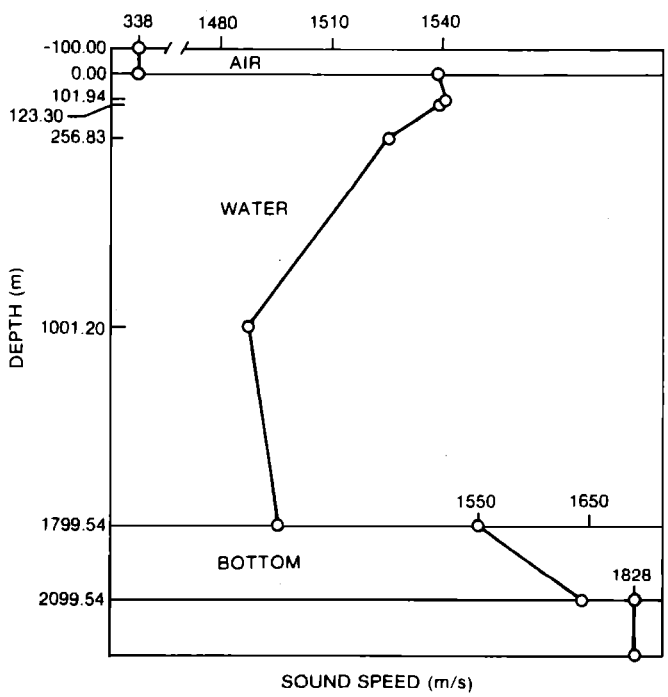

FIG. 2. Sound speed profile for examples 1 and 2.

TABLE I. Environmental and related FFP values, examples 1–3.

Layer	Depth (m) top of layer	Depth (m) bottom of layer	Sound speed (m/s) top of layer	Sound speed (m/s) bottom of layer	Sound speed type (1 = exponential 2 = constant)	H_k or p_k [Eq. (54)]	Density
0	$-\infty$	$z_1 = 0$	$C_0 = 338$	$C_0 = 338$	2	Not applicable	$\rho_0 = 0.001\,292\,84$
1	z_1	$z_2 = 101.934$	$C_1(z_1) = 1538.72$	$C_1(z_2) = 1540.83$	1	$p_1 = 2$	$\rho_1 = 1$
2	z_2	$z_3 = 123.304$	$C_2(z_2) = 1540.83$	$C_2(z_3) = 1539.06$	1	$p_2 = 8$	$\rho_2 = 1$
3	z_3	$z_4 = 256.824$	$C_3(z_3) = 1539.06$	$C_3(z_4) = 1525.31$	1	$p_3 = 10$	$\rho_3 = 1$
4	z_4	$z_5 = 1001.21$	$C_4(z_4) = 1525.31$	$C_4(z_5) = 1487.62$	1	$p_4 = 5$	$\rho_4 = 1$
5	z_5	$z_6 = 1799.54$	$C_5(z_5) = 1487.62$	$C_5(z_6) = 1495.62$	1	$p_5 = H_{\max} = 0.148\,762\,05 \times 10^6$	$\rho_5 = 1$
6	z_6	$z_7 = 2099.54$	$C_6(z_6) = 1550$	$C_6(z_7) = 1646.67$	1	$p_6 = 30$	$\rho_6 = 1.6$
7	z_7	$z_8 = \infty$	$C_7(z_7) = 1828.8$	$C_7(\infty) = 1828.8$	2	Not applicable	$\rho_7 = 2.0$

Table I. The density is assumed constant within each layer; hence, $k_{\text{eff}}^{(s)}$ reduces to the usual depth-dependent wavenumber. The sound speed variation between z_1 and z_6 is representative of conditions found during the winter in the vicinity of the Bahama Islands. The water depth of 1799.54 m is neither deep nor shallow. The environmental parameters used in the bottom ($z > z_6$) are not necessarily realistic.

The propagation loss was calculated from the ratio of the time-averaged intensity at the source, assuming that it is in a "free field" to the time-averaged intensity at the receiver. If the radial particle velocity and the pressure are approximately related by the plane wave characteristic impedance, the expression for propagation loss referenced to 1 m is

$$N_w = -20\log|\Phi(z_s, z, r)| + 10\log\left(\frac{\rho_{LR}(z)C_{LR}(z)}{\rho_{LS}(z_s)C_{LS}(z_s)}\right).$$

A. Example 1—Air to water

A 16-Hz cw source was located at -100 m in air ($z < z_0$, $LS = 0$) and the receiver was put at 15.2 m ($z_0 \leq z \leq z_1$, $LR = 1$). The pertinent parameters for the FFP were

$$\Delta\xi = 1/H_{\max} = 0.672\,214\,45 \times 10^{-5}, \quad \xi_0 = \Delta\xi$$

$$\Delta r = 114.099\,06 \text{ m}, \quad r_0 = \Delta r.$$

The number of samples required, Eq. (55) with $C_{\min} = 338$, is about 44 000 which exceeds the maximum computer array size. This problem was circumvented by collapsing[28] the required number of samples, which need not be a power of 2, down to a manageable array size of 8192. A collapsing factor of 20, i.e., (20 × 8192) total points, was used. This was excessive since a collapsing factor of 6 would have sufficed. A partial plot of $G(z_s, z; \xi_m)\xi_m^{1/2}$ versus ξ_m is shown in Fig. 3. Each peak in this plot corresponds to the presence of a singularity of G at some complex value (due in part to attenuation) of ξ. The wavenumbers associated with the sound speeds in the water column lie between $k(z_2)$ and $k(z_5)$. which are marked on the figure. It is evident that the trapping of energy within the water column itself plays an insignificant role and that the bottom bounce contribution [$0 \leq \xi \leq k(z_6)$] dominates. The solitary peak to the right occurs at a wavenumber slightly less than that associated with the sound speed in air.

The propagation loss versus range is shown in Fig. 4. It behaves as might be expected for a bottom-limited

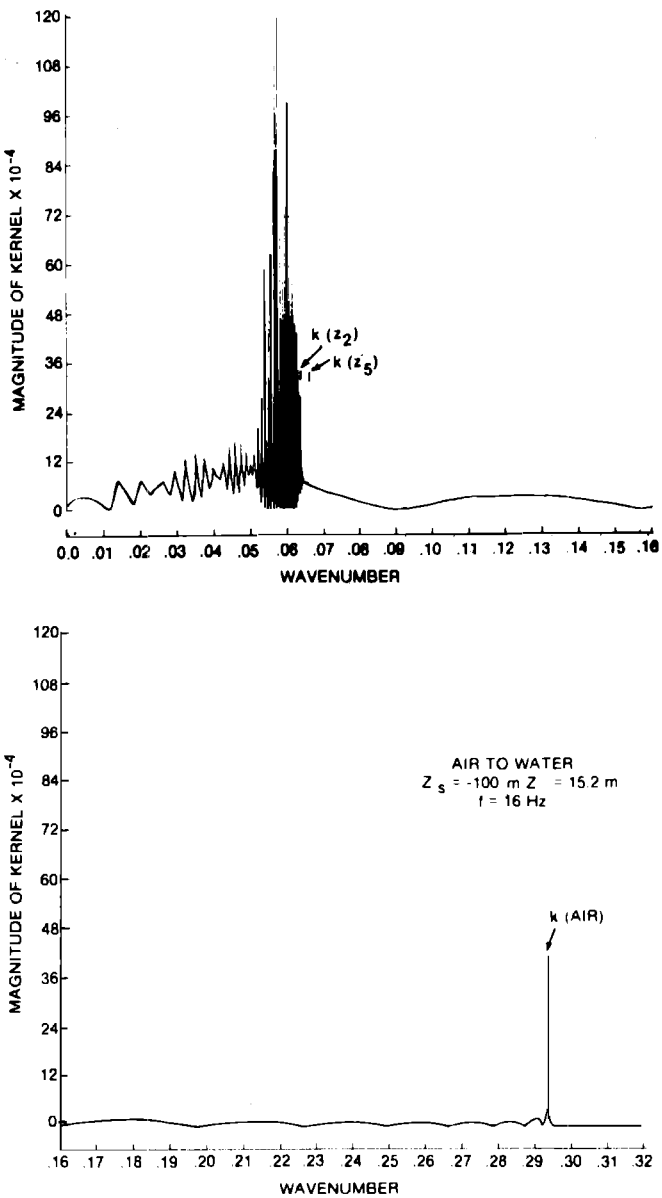

FIG. 3. Magnitude of kernel versus wavenumber for example 1.

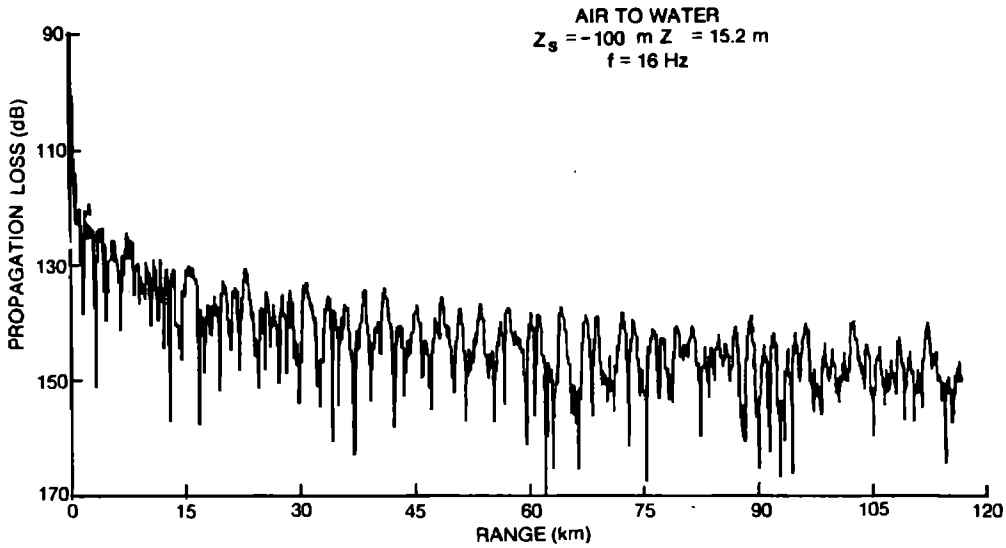

FIG. 4. Propagation loss versus range for example 1.

situation, except for the high initial loss due to the mismatch in impedance between air and water.

B. Example 2—Water to bottom

In this case the 16-Hz cw source is located in the surface duct $z_s = 15.2$ m, $LS = 1$. The receiver is placed in the bottom at $z = 1850$ m, $LR = 6$ where a sound speed gradient exists.

The distinguishing feature of the kernel versus wavenumber plot, Fig. 5, is the absence of the peak corresponding to the wavenumber in air. Figure 6 offers an examination of the propagation loss versus range for this source and receiver configuration. The figure reveals no significant difference from what would be obtained if the receiver were in the water column, with the exception of the high initial loss at close ranges.

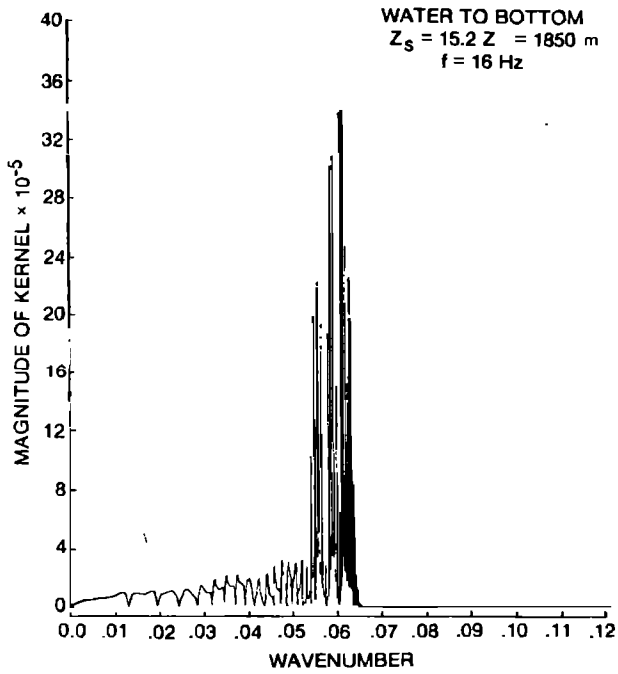

FIG. 5. Magnitude of kernel versus wavenumber for example 2.

C. Example 3—Cross layer

The source has once again been placed in the surface duct ($LS = 1$) at $z_s = 15.2$ m, but in this instance the receiver is located just below the duct ($LR = 2$) at $z = 110$ m; the frequency has been increased to 1000 Hz. The resulting propagation loss versus range is given in Fig. 7, where the unusually low propagation loss in the bottom bounce region is due to the unrealistic nature of the bottom at this frequency.

V. SUMMARY

An explicit general representation for the depth-dependent Green's function occurring in the integral solution to the wave equation has been derived. This representation permits the monochromatic point source and receiver to be located at any two depths in a plane multilayered medium. An example of its use to underwater acoustics is provided by modeling the sound speed within the air, water, and bottom with a combination of layers which have either constant or exponential sound speed variation. In addition, a technique for the evaluation of the integral solution, the Fast Field Program (FFP), has been delineated and applied to obtain answers for the propagation loss versus range resulting when:

(a) The source is in the air and the receiver is in the water;

(b) The source is in the water and the receiver is in the bottom;

(c) Both source and receiver are in the water in a cross-layered juxtaposition.

ACKNOWLEDGMENT

This work was supported by the Naval Sea Systems Command (Code SEA 06H1-4, A. P. Franceschetti, Program Manager) under Navy Subproject # SF 52 552 601-19325.

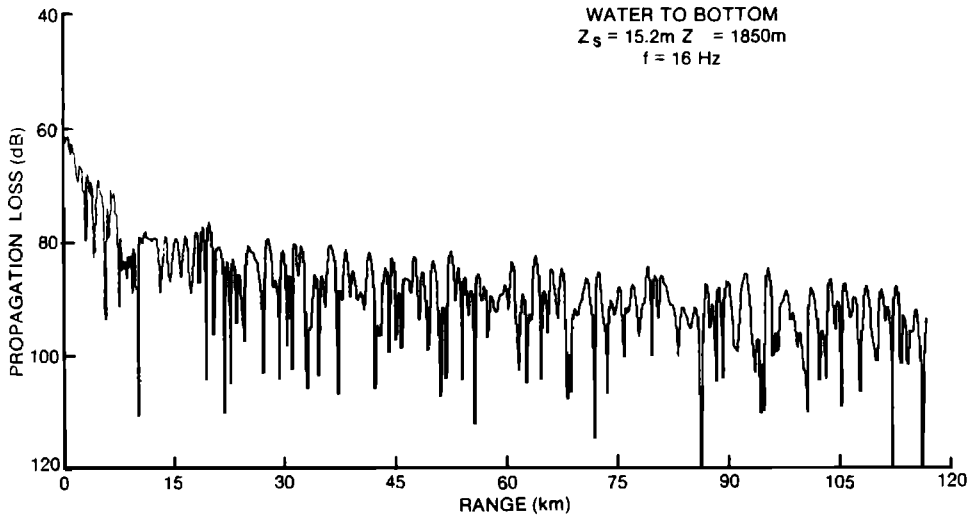

FIG. 6. Propagation loss versus range for example 2.

APPENDIX A: SPECIAL CASES FOR $G(z,z_s)$ NOT COVERED BY EQ. (46)

Explicit results for the depth-dependent Green's function are given for the case of either the source or receiver in the zero or Nth half-space. These results are derived in the same manner used to obtain Eq. (46) but that result does not reduce to the equations below because of an indexing inconsistency. In each instance, it is assumed that $z > z_s$ and the quantities are as defined in Sec. II.

Case 1. $LS = 0,\ 1 \leq LR \leq N-1$.

$$G(z,z_s) = \left[\frac{ie^{-i\beta_0 z_s}}{\beta_0}\right]\frac{[Z^{LR+1}_{LR+1}Q_{LR}(d,b)+P_{LR}(d,b)]\Delta^{LR}_{LS+1}}{(Z^1_1-\tilde{Z}^1_0)/(i\omega\rho_0)}.$$

Case 2. $1 \leq LS \leq N-2,\ LR = N$

$$G(z,z_s) = \frac{[\tilde{Z}^{LS+1}_{LS}Q_{LS}(e,b)+P_{LS}(e,b)]e^{i\beta_N(z-z_N)}Z^N_N\Delta^{N-1}_{LS+1}}{(Z^{LS+1}_{LS+1}-\tilde{Z}^{LS+1}_{LS})}.$$

Case 2a. $LS = N-1,\ LR = N$

$$G(z,z_s) = \frac{[\tilde{Z}^{LS}_{LS-1}Q_{LS}(e,b)+P_{LS}(e,b)]e^{i\beta_N(z-z_N)}}{(Z^N_N-\tilde{Z}^N_{N-1})}Z^N_N.$$

Case 3. $LS = 0,\ LR = N, (N>1)$

$$G(z,z_s) = \left[\frac{ie^{-i\beta_0 z_s}}{\beta_0}\right]\frac{e^{i\beta_N(z-z_N)}}{(Z^1_1-\tilde{Z}^1_0)}Z^N_N\Delta^{N-1}_{LS+1}.$$

Case 4. $LS = LR = 0$

$$G(z,z_s) = \left[\frac{ie^{-i\beta_0 z_s}}{\beta_0}\right]\frac{[Z^1_1\cos(\beta_0 z)-i\tilde{Z}^1_0\sin(\beta_0 z)]}{(Z^1_1-\tilde{Z}^1_0)/(i\omega\rho_0)}.$$

Case 5. $LS = LR = N$

$$G(z,z_s) = \frac{[\tilde{Z}^N_{N-1}\cos\beta_N(z_s-z_N)+iZ^N_N\sin\beta_N(z_s-z_N)]}{(Z^N_N-\tilde{Z}^N_{N-1})/(i\omega\rho_N)} \times\left[\frac{-ie^{i\beta_N(z-z_N)}}{\beta_N}\right],$$

where $d=\gamma^z_{LS}$, $e=\gamma^s_{LS}$, and $b=\gamma^{LS+1}_{LS}$ in the above special cases.

APPENDIX B: AN ALTERNATIVE NUMERICAL EVALUATION SCHEME FOR BESSEL TRANSFORMS

The observation that the Fast Fourier Transform (FFT) algorithm could be used to evaluate Bessel

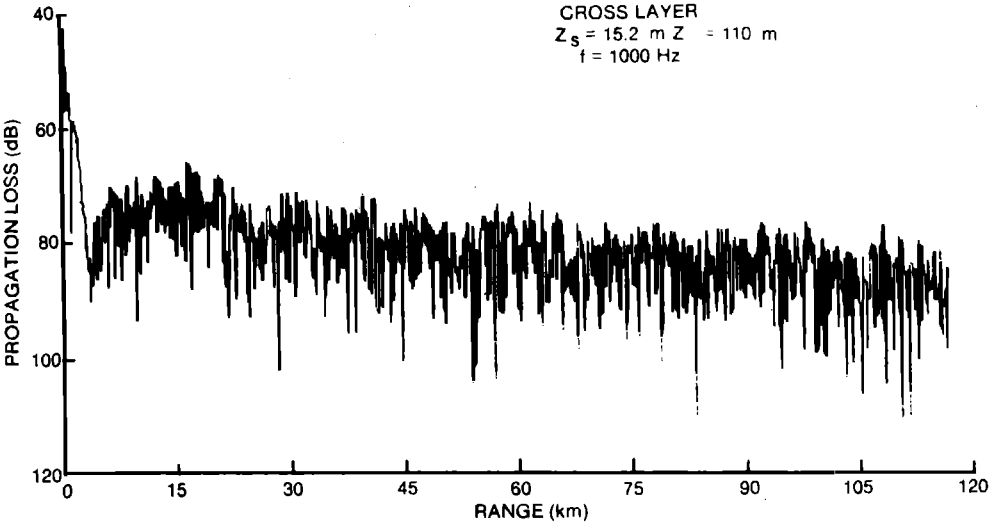

FIG. 7. Propagation loss versus range for example 3.

transforms was first made by H. W. Marsh in 1967. In his approach, the Hankel function is replaced by its large argument (ξr) asymptotic expansion. Small values of r correspond to close proximity to the source. Small values of ξ may result from either a very low frequency or from angles that are close to 90°, measured from the horizontal.

Recently, Tsang *et al.*,[29] evidently unaware of the work of Marsh, have proposed a different scheme for the evaluation of Bessel transforms, which also utilizes the FFT algorithm. The advantage of their approach is that it is exact for all values of ξr. The major disadvantage is that it requires considerably more execution time, if results are desired for more than one value of horizontal range. Their approach is used in this appendix to obtain results for the pressure field for small values of ξr, which are then compared with FFP answers.

First, we summarize the Tsang approach. The Bessel transform for the pressure field is

$$\Phi(r,z_s,z)=\frac{S_\omega}{2\pi}\int_0^\infty G(z,z_s;\xi)J_0(\xi r)\xi\,d\xi\,, \tag{B1}$$

which is recast into the equivalent form

$$\Phi(r,z_s,z)=\frac{S_\omega}{2\pi}\int_0^\infty \mathcal{G}(z,z_s;\xi)e^{-v\xi}J_0(\xi r)\xi\,d\xi\,,$$

where

$$\mathcal{G}(z,z_s;\xi)=G(z,z_s;\xi)e^{v\xi}$$

and v is a theoretically arbitrary constant, except for the restriction that $\mathrm{Re}(v)>0$. Next, we introduce the Fourier Integral Transform pairs

$$A(z,z_s;\lambda)=\int_{-\infty}^{\infty}\mathcal{G}(z,z_s;\xi)e^{-i2\pi\lambda\xi}\,d\xi$$

and (B2)

$$\mathcal{G}(z,z_s;\xi)=\int_{-\infty}^{\infty}A(z,z_s;\lambda)e^{i2\pi\lambda\xi}\,d\lambda\,.$$

The solution for the pressure field is then

$$\Phi(r,z_s,z)=\int_{-\infty}^{\infty}A(z,z_s;\lambda)I(v,\lambda,r)d\lambda\,, \tag{B3}$$

where

$$I(v,\lambda,r)=\int_0^\infty e^{-(v-i2\pi\lambda)\xi}J_0(\xi r)\xi\,d\xi$$

$$=\frac{(v-i2\pi\lambda)}{[(v-i2\pi\lambda)^2+r^2]^{3/2}}\,.$$

Evaluation of Eq. (B3) at the discrete points $\lambda_n=n\Delta\lambda$ yields

$$\Phi(r,z,z_s)\simeq\Delta\lambda\sum_{n=-L/2}^{L/2}A(n\Delta\lambda)I(v,n\Delta\lambda,r)\,,$$

where it has been tacitly assumed that contribution from the integrals corresponding to values of $|n|>L/2$ can be safely neglected. Assuming that $A(n\Delta\lambda)$ will be found from an FFT evaluation of Eq. (B2), the pressure field may be written as

$$\Phi(r,z,z_s)\simeq\Delta\lambda\left[A(0)\frac{v}{(v^2+r^2)^{3/2}}+A\left[\frac{L\Delta\lambda}{2}\right]\frac{(v+i\pi L\Delta\lambda)}{[(v+i\pi L\Delta\lambda)^2+r^2]^{3/2}}\right]+\Delta\lambda\sum_{n=1}^{L/2-1}\left[A(n\Delta\lambda)I(v,r,n\Delta\lambda)+A(L-n^1\Delta\lambda)^{1/2}I^*(v,r,n\Delta\lambda)\right], \tag{B4}$$

where the asterisk denotes the complex conjugate. Equation (B4) is valid for any r, but for each different r it must be recalculated.

1. Example B1: Inverse solution for direct path (infinite cw)

The simplest problem in underwater acoustics is to solve for the pressure field produced by a point monochromatic source located in an infinite constant sound speed ocean. The inverse of this problem from Eq. (B1) is

$$G(z,z_s;\xi)-G^*(z,z_s;\xi)$$

$$=\int_0^\infty\left(\mathrm{Im}\frac{2\pi}{i\omega\rho S_\omega}\Phi(r,z,z_s)\right)J_0(\xi r)r\,dr\,, \tag{B5}$$

where

$$P(r,z,z_s)=\frac{i\omega\rho S_\omega}{4\pi}\,\frac{e^{i\hat{k}_0R}}{R}\,,\quad R=[r^2+(z-z_s)^2]^{1/2}\,,$$

and, to an excellent approximation,

$$\hat{k}_0\simeq k_0+i\alpha\,.$$

The depth-dependent Green's function is

$$G(z,z_s;\xi)=ie^{i(z-z_s)\beta}/2\beta\,,$$

where

$$\beta=\begin{cases}\beta_1+i\beta_2, & k_0>(\xi^2+\alpha^2)^{1/2}\,,\\ \beta_2+i\beta_1, & k_0<(\xi^2+\alpha^2)^{1/2}\,,\end{cases}$$

$$\beta_2=\frac{k_0\alpha}{\beta_1}\,,\quad \beta_1=\left[\frac{[(k_0^2-\alpha^2-\xi^2)^2+4k_0^2\alpha^2]^{1/2}+|k_0^2-\alpha^2-\xi^2|}{2}\right]^{1/2}.$$

Substitution into Eq. (B5) yields

$$\frac{e^{-\beta_2(z-z_s)}}{(\beta_1^2+\beta_2^2)^{1/2}}[\cos\beta_1(z-z_s)-\phi]\,,\quad k_0>(\xi^2+\alpha^2)^{1/2}$$

$$=\int_0^\infty\frac{\sin(k_0R)e^{-\alpha R}}{R}J_0(\xi r)r\,dr$$

$$\frac{e^{-\beta_1(z-z_s)}}{(\beta_1^2+\beta_2^2)^{1/2}}\cos[\beta_1(z-z_s)-\phi]\,,\quad k_0<(\xi^2+\alpha^2)^{1/2}\,, \tag{B6}$$

where

$$\phi=\tan^{-1}(\beta_2/\beta_1)\,.$$

The integral on the right of Eq. (B6) has been evalua-

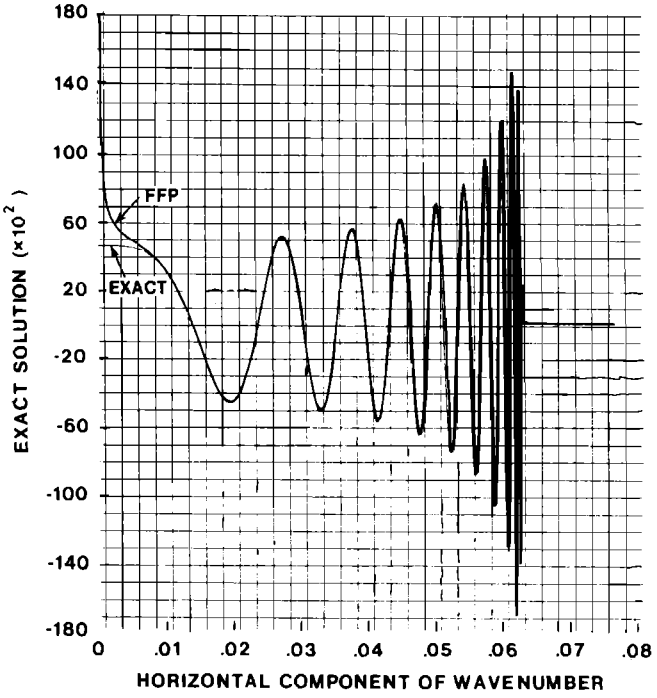

FIG. B1. Comparison of FFP and Tsang algorithms for evaluation of Eq. (B6).

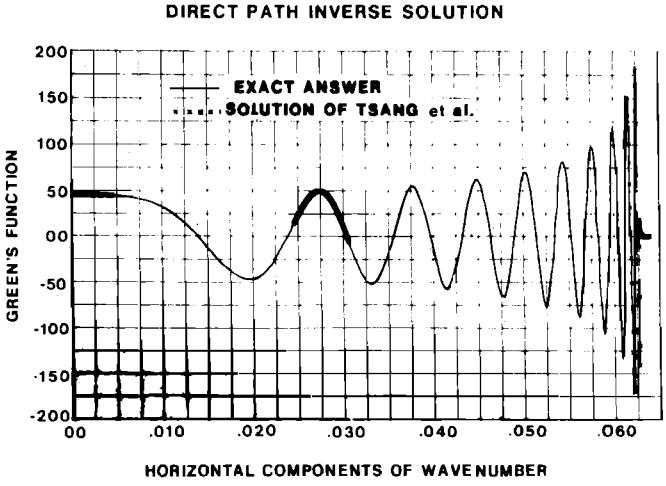

FIG. B2. Direct path inverse solution.

ted by both the FFP technique [Eq. (14)] and the Tsang algorithm [Eq. (B4)]. For the FFP evaluation, the following input values were used:

$$L = 8192, \quad k_0 = 0.062\,831\,853(\text{ft}^{-1}),$$

$$\alpha = 10^{-4}\frac{N_p}{\text{ft}}, \quad \Delta\xi = 0.306\,796\,16 \times 10^{-4}(\text{ft}^{-1}),$$

$$z - z_s = 100 \text{ ft}(30.48 \text{ m}), \quad \Delta r = 25 \text{ ft}(7.62 \text{ m}),$$

$$f = 50 \text{ Hz}, \quad \xi_0 = \Delta\xi, \quad r_0 = \Delta r.$$

The FFP answers are plotted along with the exact answers in Fig. B1. It is evident that excellent agreement exists everywhere, except for small values ($\xi < 0.01$) of ξ. This error is due to the assumption that the large argument asymptotic approximation was reasonable for all values of ξ.

The same values for the parameters listed above were used in the evaluation of the Tsang algorithm, with the exception that r_0 and ξ_0 were set equal to zero. The FFT provides results for $A(z, z_s, n\Delta\lambda)$ at the points $\lambda_n = n\Delta\lambda$, where $\Delta\lambda = (L\Delta r)^{-1}$. The proper selection for the value of v is critical to the success of this scheme. If $vr > \alpha R$, the Fourier Integral Transform for $A(z, z_s, \lambda)$ will not converge. On the other hand, the numerical results become unstable if v is extremely small. For this case, a value of $v = \alpha/2$ worked nicely. Equation (B4), with r and ξ interchanged, was evaluated at $\xi_m = m\Delta\xi$ to obtain a comparison at more than one point. The answers for various intervals of ξ_m are plotted in Fig. B2, along with the exact answers. Excellent agreement is observed for all values of ξ, including those close to $\xi = 0$ as was expected.

2. Example B2: Direct solution with multipath (infinite cw)

Both approaches are used to evaluate the received pressure field [Eq. (B1)] for a 35-Hz source located at 80 ft (24.38 m), $LS = 1$ and a receiver at 450 ft (137.16 m), $LR = 2$. A pressure release condition, $\tilde{Z}_0^1 = 0$, has been imposed at $z_1 = 0$. The pertinent environmental and related FFP values are listed in Table B1. The parameter values for the FFT are

$$L = 8192, \quad \Delta\xi = 2/H_2 = 0.277\ldots \times 10^{-5} \times (2),$$

$$\Delta r = 69.029\,135, \quad \xi_0 = \Delta\xi, \quad r_0 = \Delta r/2.$$

The FFP propagation loss (reference to 1 ft) versus range is shown in Fig. B3. The propagation loss obtained by the Tsang approach with $v = 200$ for two range intervals is shown in Figs. B4 and B5, where the FFP answers for the same range points have also been pro-

TABLE BI. Environmental and related FFP values, example B2.

Layer	Depth (ft) top of layer	Depth (ft) bottom of layer	Sound speed (ft/s) top of layer	Sound speed (ft/s) bottom of layer	Sound speed type (1 = exponential 2 = constant)	H_k or p_k [Eq. (54)]	Density
0	$-\infty$	$z_1 = 0$	Arbitrary	Arbitrary	Not applicable	Not applicable	$\rho_0 = 0$
1	z_1	$z_2 = 200$ ft	$C_1(z_1) = 5040$	$C_1(z_2) = 4956.7$	1	$p_1 = -30$	$\rho_1 = 1$
2	z_2	$z_3 = 9000$ ft	$C_2(z_2) = 4956.7$	$C_2(z_3) = 5079.4$	1	$H_2 = H_{\max} = 3.6 \times 10^5$	$\rho_2 = 1$
3	z_3	$z_4 = 9200$ ft	$C_3(z_3) = 5250$	$C_3(z_4) = 5250$	2	Not applicable	$\rho_3 = 1.5$
4	z_4	∞	$C_4(z_4) = 5425$	$C_4(\infty) = 5425$	2	Not applicable	$\rho_4 = 1.5$

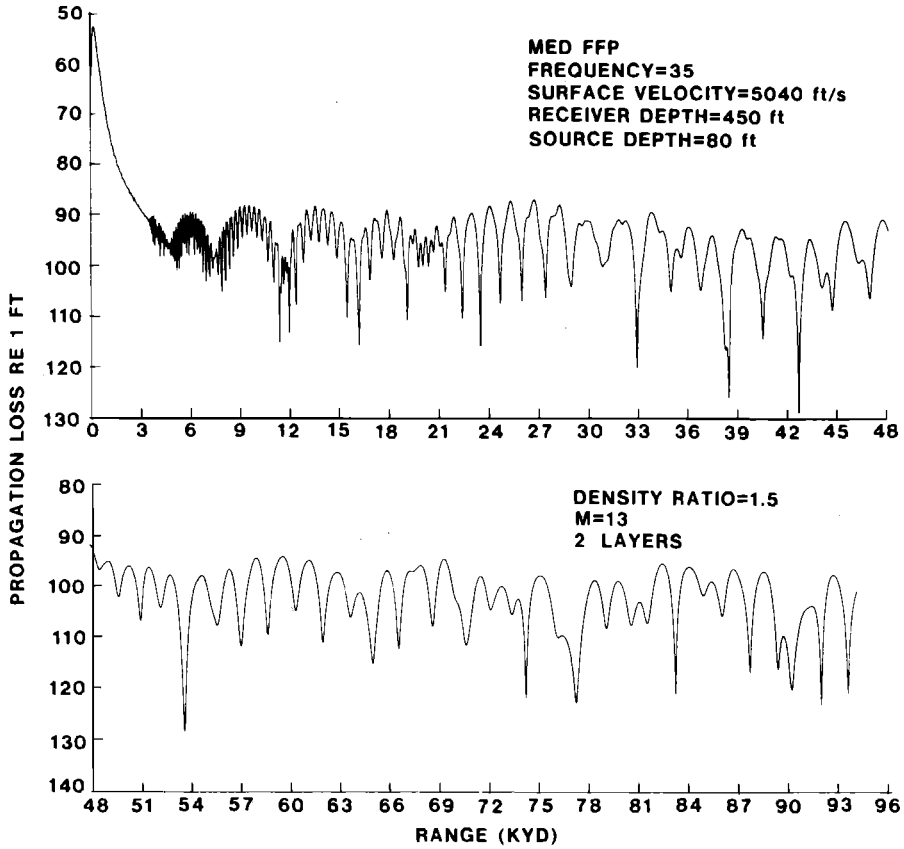

FIG. B3. Propagation loss versus range for example B-2/FFP method.

vided for comparison.

The results for Fig. B4 start at the value $r_0 = 69.029$ ft (21.04 m). The dominant paths, as given by ray theory at the beginning of the range interval, would be a direct and a surface-reflected path. The destructive interference of these two paths is responsible for the null in the pattern at very close ranges. The angles associated with these paths are small as measured from the horizontal. Thus, excellent agreement exists between the two solutions. As the range increases, the two rays merge and a shadow zone develops, which accounts for the monotonic increases in propagation loss. The pattern is interrupted at the range where significant bottom bounce energy reaches the receiver. This energy is associated with steep angles (i.e., small values of ξ) and a difference is evident between the two results. This small difference most likely can be attributed to the introduction of the asymptotic expansion in the FFP approach.

The results in Fig. B5 correspond to a range interval where bottom bounce energy predominates. However,

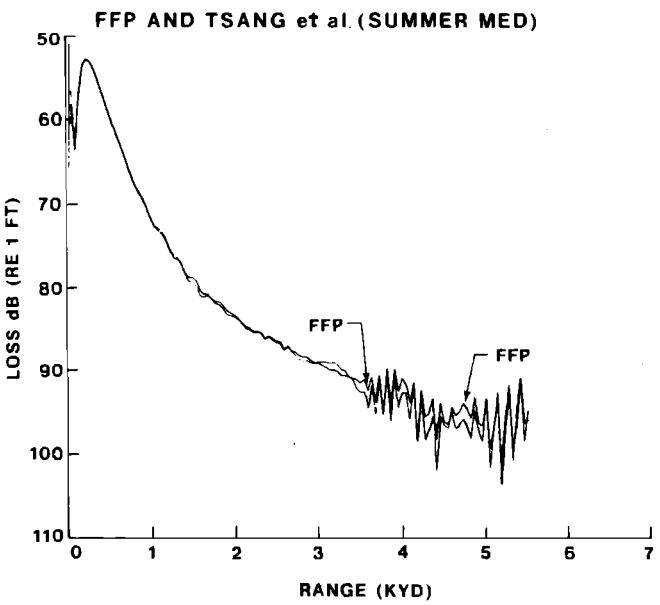

FIG. B4. Propagation loss versus range for example B-2/FFP and Tsang methods.

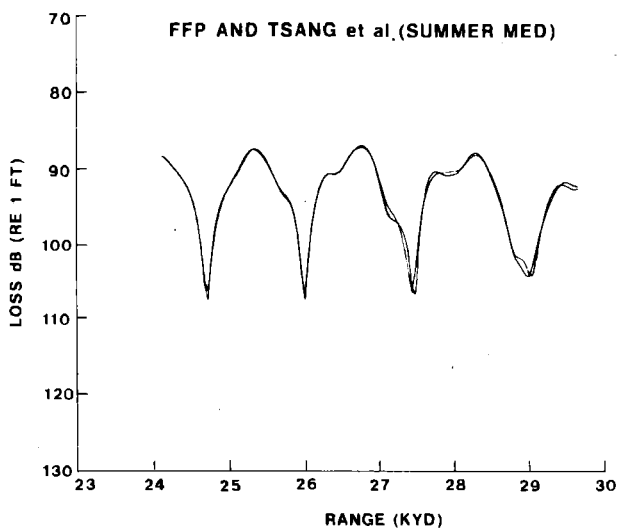

FIG. B5. Propagation loss versus range for example B-2/FFP and Tsang methods.

the corresponding values of ξ would be larger than in the previous example; thus, the agreement between the two results should be closer. An examination of the figure reveals that this is the case.

The execution time (UNIVAC 1108) required for each scheme is summarized below.

Function	Execution time (s) Tsang *et al.*	FFP
Generation of input for FFT (8192) points	101.78	104.64
Calculation of propagation loss	3.41/point	4.23 (8192 points)
Total time (4096) points	140.6914×10^2	108.87

The only approximation made in deriving the FFP is the use of the large argument asymptotic expansion for the Hankel function. This will result in some discrepancies at very close ranges to the source for some cw applications, but not for all. Such factors as source and receiver depths, sound speed variation, frequency, and boundary losses have a significant bearing on whether or not the discrepancy will exist. For very close range cw applications, the uncertainty could be removed by using the formulation of Sec. II in conjunction with Eq. (B4). This approach should be taken for close range pulse propagation problems, such as multichannel seismic reflection schemes, in which near-normal incident returns can be separated in time from the shallow angle water refracted and reflected arrivals.

[1]J. E. Freehafer, "Physical Optics," in *Propagation of Short Radio Waves*, edited by D. E. Kerr, MIT Radiation Laboratory Series (McGraw–Hill, New York, 1951), Vol. 13, pp. 58–70.

[2]L. B. Felsen and N. Marcuvitz, *Radiation and Scattering of Waves* (Prentice–Hall, Englewood Cliffs, NJ, 1973).

[3]J. R. Wait, *Electromagnetic Waves in Stratified Media* (Pergamon, New York, 1970).

[4]D. G. Harkrider, "Theoretical and Observed Acoustic-Gravity Waves from Explosive Sources in the Atmosphere," J. Geophys. Res. 69, 5295–5321 (1964).

[5]H. W. Kutschale, "Further Investigation of the Integral Solution of the Sound Field in Multilayered Media: A Liquid-Solid Half Space With a Solid Bottom," Technical Report CU-6-71, Lamont-Doherty Geological Observatory of Columbia University, Palisades, NY (March 1972).

[6]L. M. Brekhovskikh, *Waves in Layered Media* (Academic, New York, 1960).

[7]D. C. Stickler, "Normal-Mode Program with Both the Discrete and Branch Line Contributions," J. Acoust. Soc. Am. 57, 856–861 (1975).

[8]H. W. Marsh and S. R. Elam, Internal Document, Raytheon Co., Marine Research Laboratory, New London, CT (1967).

[9]F. R. DiNapoli, "A Fast Field Program for Multilayered Media," NUSC Technical Report 4103 (1971).

[10]P. M. Morse and K. U. Ingard, *Theoretical Acoustics* (McGraw–Hill, New York, 1968), pp. 309–312.

[11]A. Sommerfeld, "Über die Ausbreitung der Wellen in der drahtlosen Telegraphie," Ann. Physik 28, 665–736 (1909).

[12]H. Lamb, "On the Propagation of Tremors Over the Surface of an Elastic Solid," Phil. Trans. R. Soc. London Ser A 203, 1–42 (1904).

[13]E. C. Titchmarsh, "A Relation Between Green's Functions," J. London Math. Soc. 26, 31–36 (1951).

[14]I. Tolstoy, *Wave Propagation* (McGraw–Hill, New York, 1973).

[15]B. Van der Pol and H. Bremer, "The Diffraction of Electromagnetic Waves from an Electrical Point Source Round a Finitely Conducting Sphere, with Applications to Radiotelegraphy and the theory of the Rainbow," Phil. Mag. 24, 141–176 and 825–863 (1937).

[16]P. Debye, "Das elektromagnetische Feld um einen Zylinder und die Theorie des Regenbogens," Phys. Z. 9, 775–778 (1908).

[17]J. R. Wait, "A Diffraction Theory for LF Sky-Wave Propagation," J. Geophys. Res. 66, 1713–1730 (1961).

[18]D. V. Batorsky and L. B. Felsen, "Ray-Optical Calculation of Modes Excited By Sources and Scatterers in a Weakly Inhomogeneous Duct," Radio Sci. 6, 911–923 (1971).

[19]G. A. Leibiger and D. Lee, "Application of Normal Mode Theory to Convergence Zone Propagation," Vitro Laboratory Res. Memorandum VL-8512-12-0, Vitro Laboratories, West Orange, NJ (30 November 1968).

[20]H. Weinberg, "Application of Ray Theory to Acoustic Propagation in Horizontally Stratified Oceans," J. Acoust. Soc. Am. 58, 97–109 (1975).

[21]H. F. Baker, "On the Integration of Linear Differential Equations," Proc. London Math. Soc. Ser. 1 35, 333–378 (1902).

[22]R. A. Frazer, W. J. Duncan, and A. R. Collar, *Elementary Matrices* (Cambridge U.P., London, 1960).

[23]F. R. Gantmacher, *The Theory of Matrices* (Chelsea, New York, 1959), Vol. 2, pp. 125–135.

[24]F. Gilbert and G. E. Backus, "Propagator Matrices in Elastic Wave and Vibration Problems," Geophysics 31, 326–332 (1966).

[25]G. Peano, "Intégration par Series des Équations Différentielles Linéaires," Math. Ann. 32, 450–456 (1888).

[26]E. A. Coddington and N. Levinson, *Theory of Ordinary Differential Equations* (McGraw–Hill, New York, 1955), pp. 246–252.

[27]F. R. DiNapoli and M. R. Powers, "Recursive Calculation of Products of Cylindrical Functions," NUSC Technical Memorandum No. PA-83-70 (1970).

[28]F. R. DiNapoli, "The Collapsed Fast Field Program (FFP)," NUSC Technical Memorandum No. TA11-317-72 (1972).

[29]L. Tsang, R. Brown, J. A. Kong, and G. Simmons, "Numerical Evaluation of Electromagnetic Fields Due to Dipole Antennas in the Presence of Stratified Media," J. Geophys. Res. 79, 2077–2080 (1974).